Supporting Information

A fluorescent probe based on enhanced ICT effect for Hg^{2+} detection and cell imaging

Shuchen Pei [a], Chaozheng Li [a], Xinyu Pei [a], Xiangyang Zhang [b],Yuting Chi [a], Wenhong Zeng [a], Yuanyuan Zhang [c], Xiaoling Liao *[c] and Jun Chen * [a]

[a] School of Chemistry and Chemical Engineering, Chongqing University of Science and Technology, Chongqing, 401331, China.

[b] College of Chemistry and Chemical Engineering, Hunan University of Arts and Science, Changde 415000, China

[c] School of Metallurgy and Materials Engineering, Chongqing University of Science and Technology, Chongqing, 401331, China.

* Corresponding authors: E-mail address: wxchenjun@163.com

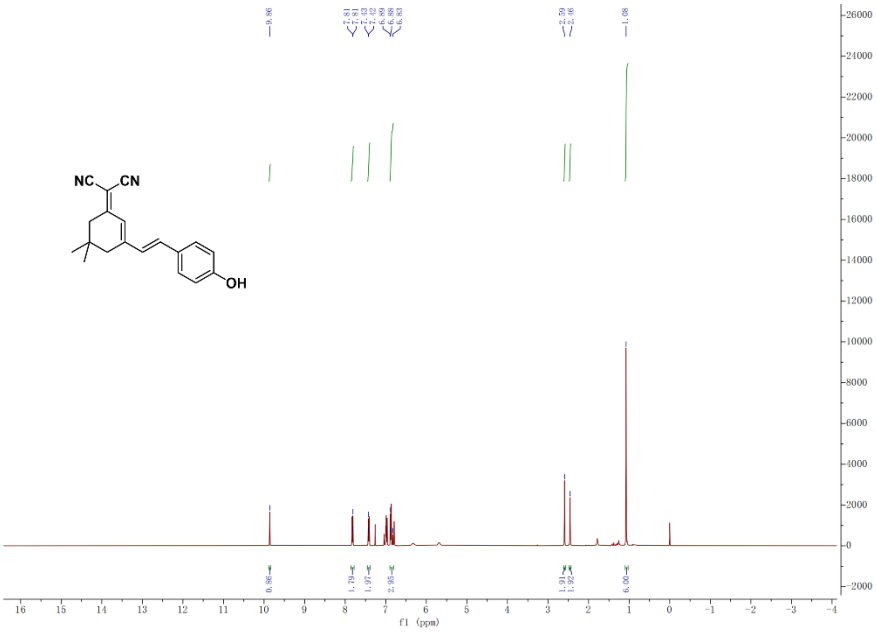

Fig. S1 ^{1}H NMR spectrum of **YF-OH** (400 MHz, $CDCl_3$).

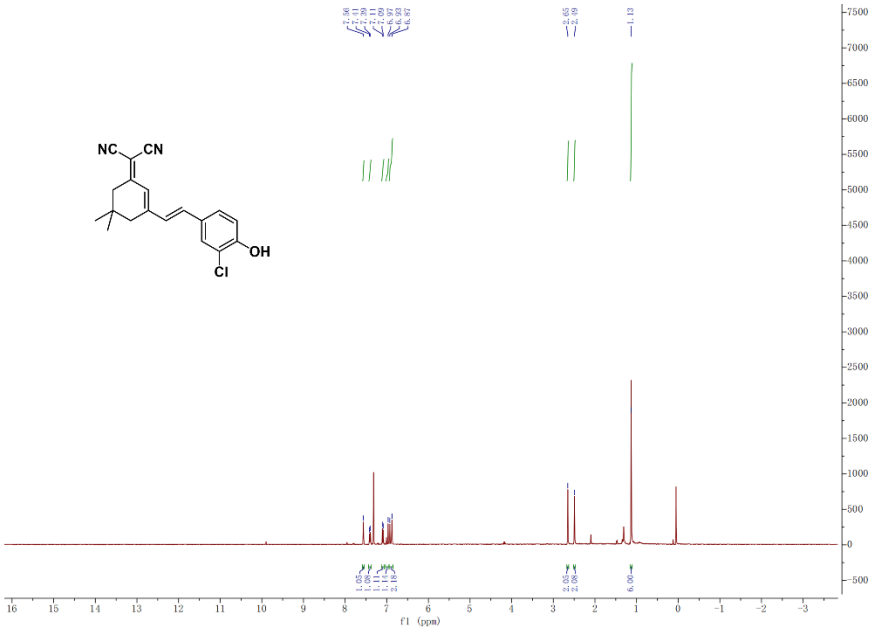

Fig. S2 ^{1}H NMR spectrum of **YF-Cl-OH** (400 MHz, $CDCl_3$).

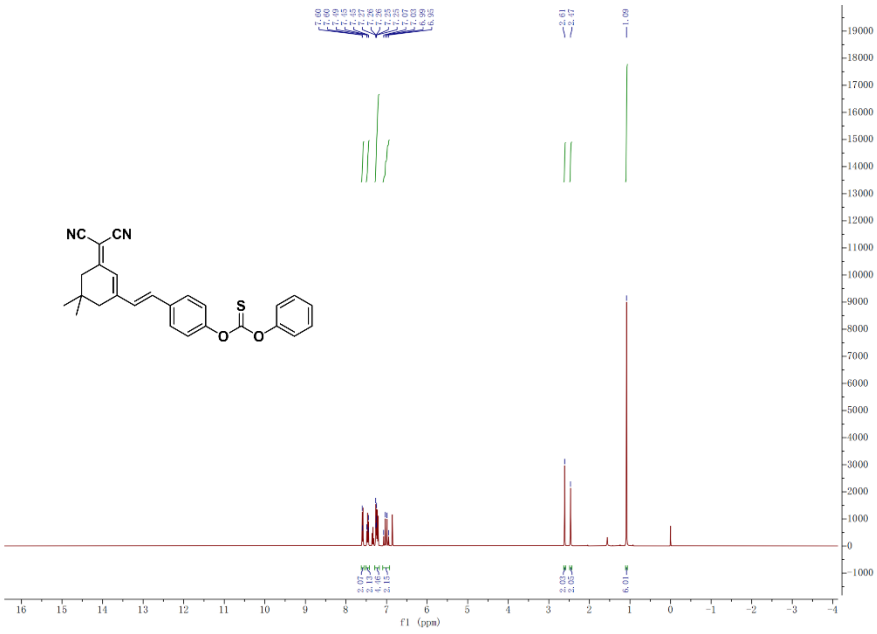

Fig. S3 ^{1}H NMR spectrum of **YF-Hg** (400 MHz, $CDCl_3$).

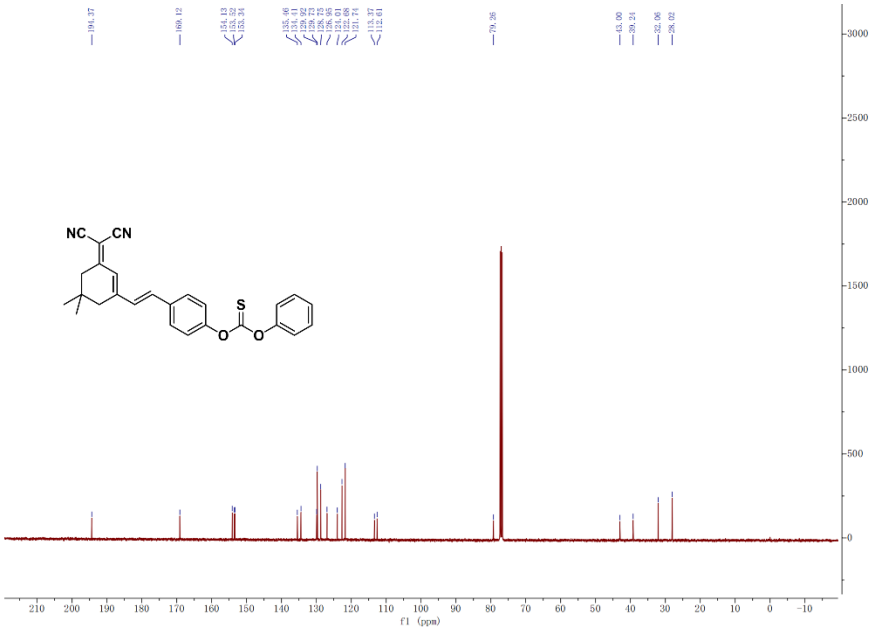

Fig. S4 ^{13}C NMR spectrum of **YF-Hg** (101 MHz, $CDCl_3$).

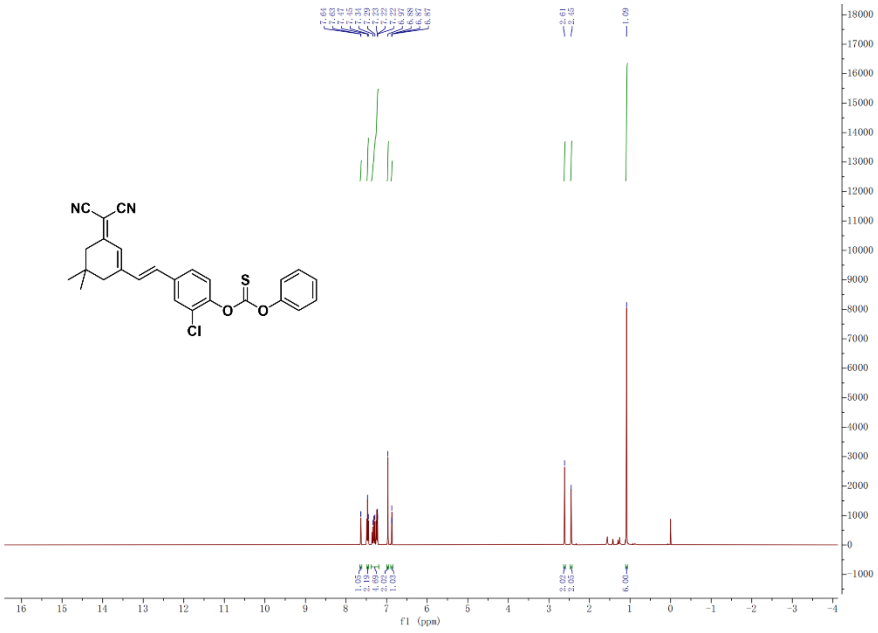

Fig. S5 ^{1}H NMR spectrum of **YF-Cl-Hg** (400 MHz, $CDCl_3$).

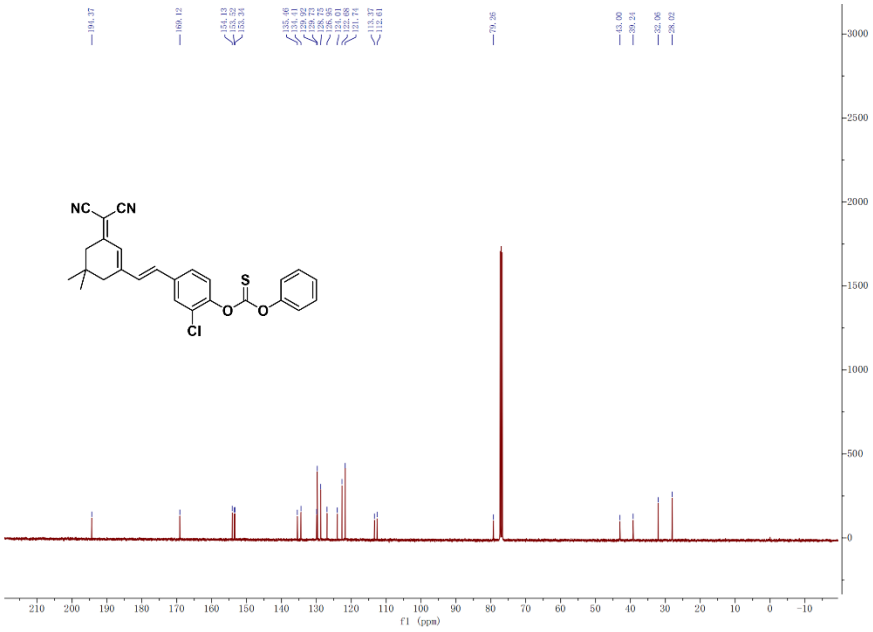

Fig. S6 ^{13}C NMR spectrum of **YF-Cl-Hg** (101 MHz, $CDCl_3$).

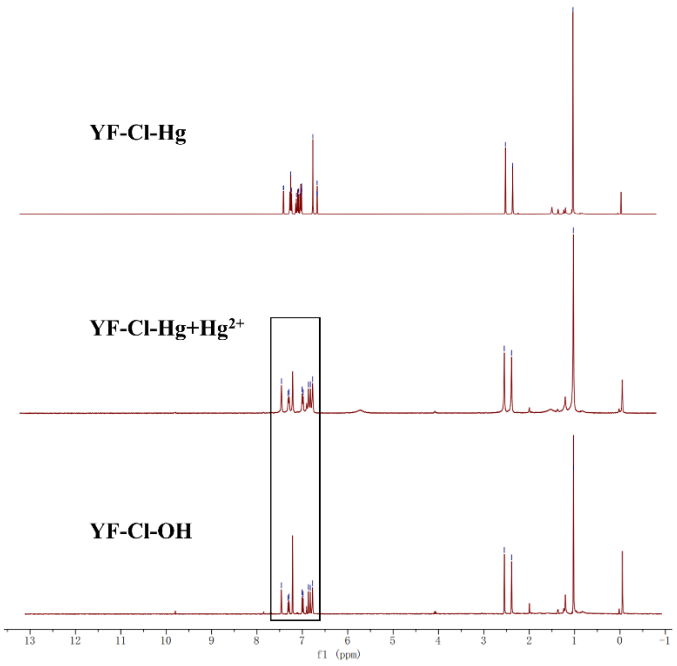

Fig. S7 Comparison of ^{1}H NMR **YF-Cl-Hg**+Hg^{2+} with **YF-Cl-Hg** and **YF-Cl-OH**.

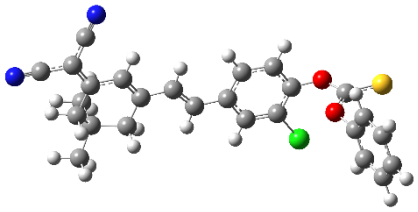

Fig. S8 Structure of **YF-Cl-Hg**.

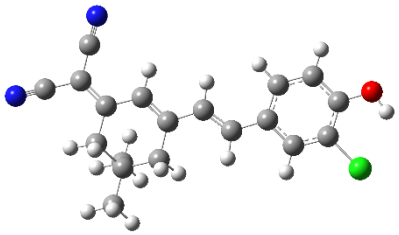

Fig. S9 Structure of **YF-Cl-OH**.

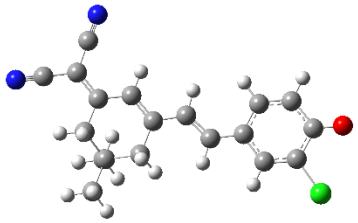

Fig. S10 Structure of **YF-Cl-O**$^{-}$.

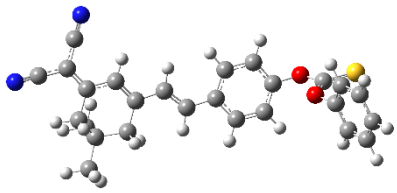

Fig. S11 Structure of **YF-Hg**.

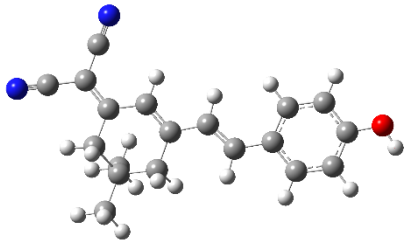

Fig. S12 Structure of **YF-OH**.

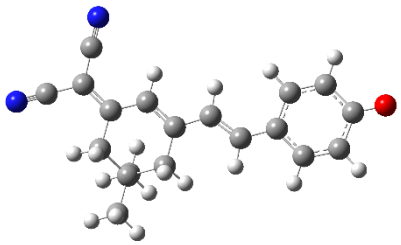

Fig. S13 Structure of **YF-O**$^{-}$.

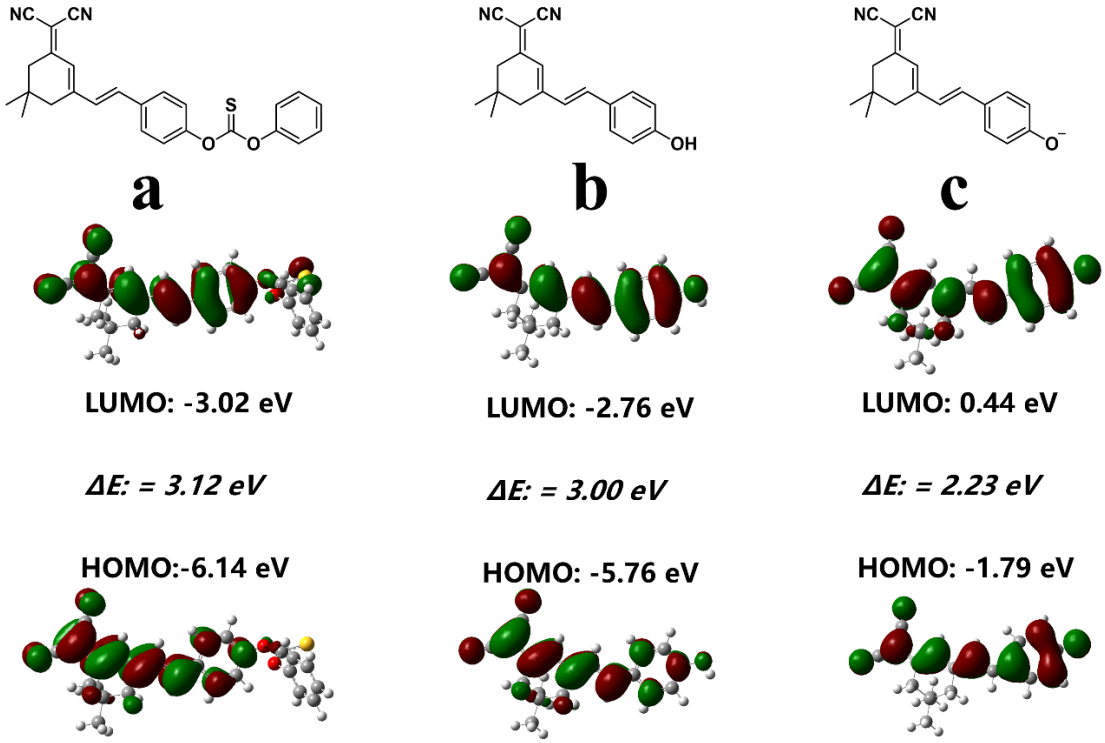

Fig. S14 Molecular front orbital diagrams of **YF-H-Hg**, **YF-H-OH** and **YF-H-O**$^{-}$.

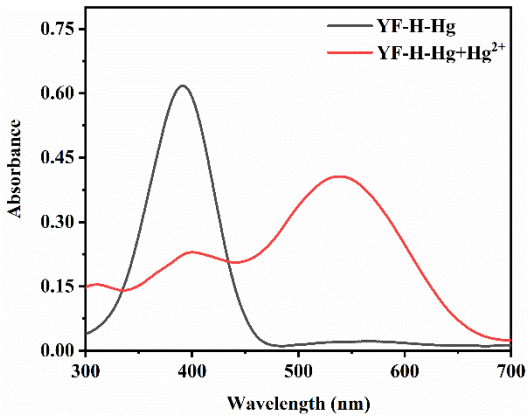

Fig. S15 Absorption spectra of **YF-Hg** in pH buffer (pH=8, contained 50% DMF) in the absence and presence of Hg^{2+} (100 μM).

As shown in Fig. 3a, the UV absorption of **YF-Hg** after responding to Hg^{2+} is only weakly red-shifted. It indicates that the HOMO-LUMO energy gap of its structure formed in response to Hg^{2+} should be slightly reduced, which is basically consistent with the DFT calculation results in Fig S14.

Meanwhile, the UV absorption spectra of **YF-Hg** at pH=8 in response to Hg^{2+} were measured. As shown in Figure S15, there is a large red shift in the UV absorption of **YF-Hg** after responding to Hg^{2+} at pH=8, which implies the formation of a **YF-O**$^{-}$ structure.

Table. S1 Comparison of **YF-Cl-Hg** with other dithioacetal-based Hg^{2+} fluorescent probes.

Probe	References	LOD for Hg^{2+}	Stocks shift (nm)	λem	Cell imaging
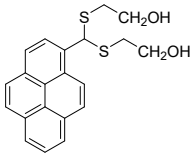	[1]	1.03×10^{-9} mol/L	62 nm	457 nm	yes
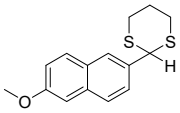	[2]	5.0×10^{-6} mol/L	112 nm	412 nm	-
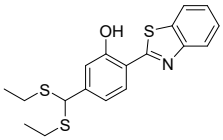	[3]	1.59×10^{-8} mol/L	103 nm	552 nm	yes
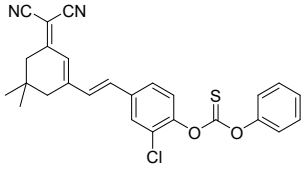	This work	5.82×10^{-7} mol/L	149 nm	659 nm	yes

Notes and references

1. Y. Y. Gao, T. T. Ma, Z. Z. Ou, W. J. Cai, G. Q. Yang, Y. Li, M. H. Xu and Q. Q. Li, *TALANTA*, 2018, **178**, 663-669.
2. J. Prabhu, K. Velmurugan and R. Nandhakumar, *Journal of Luminescence*, 2014, **145**, 733-736.
3. Y. Zhou, X. He, H. Chen, Y. Wang, S. Xiao, N. Zhang, D. Li and K. Zheng, *Sensors and Actuators B: Chemical*, 2017, **247**, 626-631.